Louisiana State University

LSU Digital Commons

4-26-2013

Inhomogeneous superconducting states of mesoscopic thin-walled cylinders in external magnetic fields

K. Aoyama
Hakubi Center for Advanced Research

R. Beaird
Louisiana State University

D. E. Sheehy
Louisiana State University

I. Vekhter
Louisiana State University

Follow this and additional works at: https://digitalcommons.lsu.edu/physics_astronomy_pubs

Recommended Citation

Inhomogeneous Superconducting States of Mesoscopic Thin-Walled Cylinders in External Magnetic Fields

K. Aoyama, R. Beaird, D. E. Sheehy, and I. Vekhter

Inhomogeneous superconducting states of mesoscopic thin-walled cylinders in magnetic fields

K. Aoyama[1,2,3], R. Beaird[2], D. E. Sheehy[2], and I. Vekhter[2]

[1] *The Hakubi Center for Advanced Research, Kyoto University, Kyoto 606-8501, Japan*
[2] *Department of Physics and Astronomy, Louisiana State University, Baton Rouge, LA 70803*
[3] *Department of Physics, Kyoto University, Kyoto 606-8502, Japan*

We theoretically investigate the appearance of spatially modulated superconducting states in mesoscopic superconducting thin-wall cylinders in a magnetic field at low temperatures. Quantization of the electron motion around the circumference of the cylinder leads to a discontinuous evolution of the spatial modulation of the superconducting order parameter along the transition line $T_c(H)$. We show that this discontinuity leads to the non-monotonic behavior of the specific heat jump at the onset of superconductivity as a function of temperature and field. We argue that this geometry provides an excellent opportunity to directly and unambiguously detect distinctive signatures of the Fulde-Ferrell-Larkin-Ovchinnikov modulation of the superconducting order.

Mesoscopic systems both serve as a platform to investigate fundamental quantum physics of solids and are a testing ground for potentially transformative future devices [1–5]. Of special interest in this context are interacting systems exhibiting interplay of the collective emergent properties with the quantum physics of single particles. Small superconducting samples of nontrivial topology provide an example of such interplay since the global phase of the pair condensate and the phases of single particle wave functions respond differently to the applied magnetic field.

In mesoscopic superconducting rings of radius $R \sim \xi_0$, where $\xi_0 \equiv v_{\mathrm{F}}/2\pi T_c(H = 0)$ is the superconducting coherence length, and v_F is the Fermi velocity, this leads to a doubling of the period of the oscillations of the transition temperature, T_c, as a function of the magnetic flux, Φ, through the ring, relative to the well-known Little-Parks (LP) effect [5, 6, 8]. The small ring radius, R, implies that each single electron state can be labeled by its angular momentum, n, in units of $\hbar$, and each particle acquires an additional phase due to the magnetic flux, $\Phi = \pi R^2 H$ when circling around the ring. In the absence of the field the wave function of the Cooper pair has a net zero angular momentum, as the time-reversed states with $n_1 = -n_2$ form a bound state. In contrast, under the applied field the non-zero quantum number $l = n_1 + n_2$ partially compensates the net flux and maximizes the transition temperature, T_c. Therefore, for a small ring [7, 8], T_c is a periodic function of $\phi = \Phi/(2\Phi_0)$ with the flux quantum $\Phi_0 = hc/2e$, while for a large ring the periodicity is solely due to the flux experienced by an electron *pair* with charge $2e$, i.e. T_c is a periodic function of Φ/Φ_0 (LP effect).

Under these assumptions, there is no overall suppression of the maximal T_c as the magnetic field increases: at integer values of ϕ the orbital coupling of the field to the individual electrons can be fully compensated by the finite angular momentum l of the Cooper pair. The de-struction of superconductivity in such a geometry must then occur via paramagnetic (Zeeman) coupling of the electron spins to the field, which raises the energy of the singlet bound state: inclusion of this coupling is essential for developing a complete picture. Consequently in this Letter we consider the combined effect of the orbital and Zeeman effect on superconductivity, and analyze a mesoscopic thin-walled cylinder with the field along the axis. The cylinder geometry allows the formation of a spatially-modulated [9, 10] (Fulde-Ferrell-Larkin-Ovchinnikov, FFLO) superconducting state that enables pairing under high Zeeman field. We show below that a) this state occurs even if the cylinder is made out of materials where superconductivity is not paramagnetically limited in the bulk; b) signatures of such a state are much more prominent and easily identified in this geometry with $R \sim \xi_0$ than either in bulk materials or flat thin films, and therefore mesoscopic systems offer a unique chance to detect the FFLO state that has remained elusive for nearly 50 years since it was first predicted.

Our main results are shown in Fig. 1. While at low fields the variation of the transition temperature $T_c(H)$ is well described by the Little-Parks (LP) periodicity, at higher fields there is an extended region in which the superconducting order parameter is modulated along the cylinder axis. Near the phase boundary $T_c(H)$ in this regime, the superconducting phase exhibits alternating regions of phase-modulated (FF) and amplitude-modulated (LO) order; however, the LO phase becomes stable at lower T. The wavevector, q_z, of this modulation has non-analytic dependence on H, due to the interplay between the finite size effects and the LP oscillations. The heat capacity jump at $T_c(H)$ varies dramatically along this sequence of transitions (in contrast to the smooth evolution at temperatures where the FFLO modulation is absent), enabling a direct identification of the modulated states.
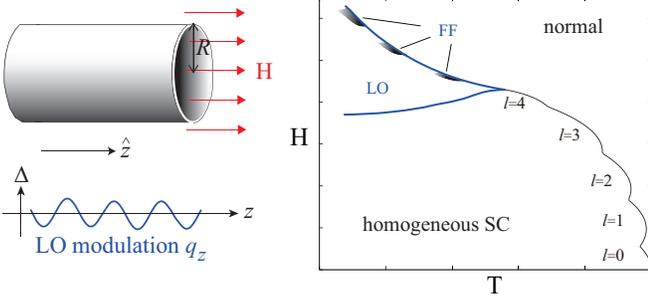
FIG. 1: (Color online) Superconducting thin-wall cylinder with a small radius R in a magnetic field parallel to the cylinder axis (z-axis). Sketch shows the spatial modulation of the order parameter in the LO phase. Right-panel: phase diagram in the H-T plane, showing regions of the normal phase, homogeneous ($q_z = 0$) superconductor, and spatially-modulated LO phase, with phase modulated FF states indicated by the shaded regions.

Although the possibility of FFLO states has been discussed in bulk materials such as the heavy-fermion superconductor CeCoIn$_5$ [11–13] and organic superconductors [14–17], it is difficult to design a "smoking gun" experiment that unequivocally points towards such a state. In real bulk systems both orbital and paramagnetic coupling suppress superconductivity, and inhomogeneity arises due to both. The former effect leads to proliferation of the vortices. Each vortex contains exactly one flux quantum for the Cooper pairs, Φ_0, which corresponds to a 2π-phase winding of the superconducting order parameter around the vortex core. In that sense a thin-walled ring or cylinder can be viewed as a coreless "supervortex" of multiple flux quanta, with a phase winding $2\pi l$. In contrast, paramagnetic pairbreaking favors FFLO states. Recall that in a singlet superconductor in the absence of Zeeman splitting the Cooper pair comprises electrons in time-reversed states, which have equal energies, and therefore are unstable towards formation of a bound state. With paramagnetic coupling the states with opposite spins have equal energies if they have a field-dependent momentum mismatch q, and the modulation of the FFLO state originates from this finite center-of-mass momentum (CMM) of the Cooper pairs. On a 1D ring the pair CMM is equivalent to the net phase winding, so that a different geometry is needed to distinguish the modulated states.

We consider a long hollow superconducting cylinder of radius R and thickness $d \ll \xi_0$, which, in the absence of a magnetic field, is described by the Hamiltonian

$$
\begin{aligned}
\mathcal{H} &= \sum_{\sigma,\boldsymbol{p}} \xi(\boldsymbol{p}) \hat{c}^\dagger_{\mathbf{p},\sigma} \hat{c}_{\mathbf{p},\sigma} - \lambda \sum_{\mathbf{q}} \hat{B}^\dagger(\mathbf{q})\, \hat{B}(\mathbf{q}),\\
\hat{B}(\mathbf{q}) &= \frac{1}{2} \sum_{\mathbf{p},\alpha,\beta} (-i\,\sigma_y)_{\alpha,\beta}\, \hat{c}_{-\mathbf{p}+\frac{\mathbf{q}}{2},\alpha} \hat{c}_{\mathbf{p}+\frac{\mathbf{q}}{2},\beta}\,.
\end{aligned} \tag{1}
$$

Here $\hat{c}_{\mathbf{p},\alpha}$ is the annihilation operator for an electron with

momentum $\mathbf{p}$ and spin projection α, λ is the strength of the pairing interaction, and we assumed singlet s-wave superconductivity. For small R the motion around the circumference of the cylinder is quantized, while the momentum along the axis (z) is continuous, so that $\mathbf{p} = (m/R, p_z)$ with m integer, and the quasiparticle energy takes the form

$$
\xi(\mathbf{p}) = \frac{1}{2M}\left[p_z^2 + \left(\frac{m}{R}\right)^2 \right] - \mu\,, \tag{2}
$$

where M is the electron mass and μ is a chemical potential. Here the summation over the momenta means $\sum_{\mathbf{p}} = \left[(2\pi)^2 R\right]^{-1} \sum_{m\in Z} \int dp_z$.

The magnetic field threading the cylinder along its axis leads to a Zeeman splitting of the single particle energy levels by $H_Z = \sum_{\sigma,\mathbf{p}} \sigma\, h\, \hat{c}^\dagger_{\mathbf{p},\sigma} \hat{c}_{\mathbf{p},\sigma}$, where $h = \mu_B\, gH$, μ_B is the Bohr magneton, and g is the g-factor of the quasiparticles in the crystal. At the same time the momentum operator has to be replaced by its gauge-invariant counterpart, $\widehat{\boldsymbol{p}} \to \widehat{\boldsymbol{p}} + |e|\boldsymbol{A}$. For our model of a thin-walled cylinder the vector potential $\mathbf{A} = -\hat{\varphi} H R/2$, and φ is the azimuthal angle around the cylinder. Hence $|\mathbf{A}| = const$ on the cylinder.

In the superconducting (SC) phase the pair field $\Delta(\mathbf{q}) = \lambda\langle \hat{B}(\mathbf{q})\rangle$, where $\langle\ldots\rangle$ denotes the thermal average, acquires a non-zero value. Due to the cylindrical geometry, $\Delta(\mathbf{r})$ can be expanded in the Fourier series,

$$
\Delta(\mathbf{r}) = |\Delta_0| \sum_{q_z} \sum_{l\in Z} C_{l,q_z} e^{i\,l\varphi} e^{i\,q_z\,z}. \tag{3}
$$

The uniform SC state at $H = 0$ only has $C_{0,0} \neq 0$, while a single component $C_{l,0}$ with flux-dependent $l \neq 0$ characterizes the SC transition under orbital coupling to the field and gives rise to the Little-Parks effect. If the cylinder were to unfold into a two-dimensional (2D) plane, l and q_z would become components of a 2D vector $\boldsymbol{q}$, and in response to a Zeeman field a state with $\boldsymbol{q} \neq 0$ would be realized. The cylindrical geometry is unique since $l \neq 0$ gives the magnetic flux through the cylinder, and therefore the FFLO modulation is only along the axis, $q_z \neq 0$. Near the transition the linearized gap equations for different l, $|q_z|$ decouple [18, 19], and hence superconducting states appear either with a single $C_{l,\boldsymbol{q}_z}$ (phase modulated, $\Delta(\mathbf{r}) = \Delta_0 e^{il\varphi} e^{i\boldsymbol{q}_z z}$, FF), or with $C_{l,q_z} = C_{l,-q_z}$ (amplitude modulated, $\Delta(\mathbf{r}) = \Delta_0 e^{il\varphi} \cos(\boldsymbol{q}_z z)$, LO, see Fig. 1). Thus, this setting has an advantage over other ways to achieve FFLO states (such as bulk paramagnetically-limited superconductors, imbalanced fermionic atomic gases [32] or thin SC films), in which modulation direction is arbitrary, and therefore complex states may be favored [20–25].

To study the transition between the normal and SC states we use the Ginzburg-Landau (GL) expansion of the free energy, $\mathcal{F}_{GL} = a^{(2)}(l, q_z, T, H)|\Delta_0|^2 + a^{(4)}(l, q_z, T, H)|\Delta_0|^4$, At each H, l, q_z, the temperature T

where $a^{(2)}(l, q_z, T, H)$ becomes negative (if it exists) indicates a putative second order transition from the normal into the SC state with given values of l, q_z. The highest of these temperatures is the physical transition point $T_c(H)$ into a state with the corresponding l, q_z. The necessary condition for the continuous transition is that the quartic coefficient $a^{(4)}(l, q_z, T_c(H), H)$ remains positive at the transition point.

We evaluate the coefficients $a^{(2)}$ and $a^{(4)}$ using the Green's function formalism for the Hamiltonian, Eq. (1), with the Zeeman and orbital coupling terms. We note here that a similar setup was considered in Ref. 27 using a phenomenological GL expansion that is valid only in the long-wavelength modulation limit. Due to the neglect of the field dependence of the coefficients of the GL expansion, lack of connection with a microscopic model Hamiltonian, and the assumption of a small modulation wave vector, that approach failed to capture any of the physics found in this Letter, and led the authors of Ref. 27 to focus on the fluctuation contribution to the specific heat as the main observable. Our analysis below shows that the "mean field" features of the transition, when analyzed properly, strongly reflect the interplay of the quantization of single electron motion and spatial modulation of the SC order. We use a quasi-classical approximation for the

normal state Green's function $-\langle T_\tau \hat{\psi}_\sigma(\mathbf{r}, \tau) \hat{\psi}_\sigma^\dagger(\mathbf{r}', 0) \rangle \simeq T \sum_{\varepsilon_n} e^{-\varepsilon_n \tau} \mathcal{G}_{\varepsilon_n, \sigma}(\mathbf{r} - \mathbf{r}') e^{i|e| \int_{\mathbf{r}}^{\mathbf{r}'} d\mathbf{s} \cdot \mathbf{A}(\mathbf{s})}$, where the integral in the exponent is evaluated along a straight line. This approximation smears out the even-odd flux periodicity for a 1D ring, but this periodicity is already broken by Zeeman coupling, and hence the approximation is adequate for our goals. We obtain for the quadratic term

$$a^{(2)}|\Delta_0|^2 = \int d\mathbf{r}\, \Delta^*(\mathbf{r}) \Big(\frac{1}{\lambda} - \frac{T}{2} \sum_{\varepsilon_n, \sigma} \sum_{\mathbf{p}} \hat{K}(\varepsilon_n, \sigma) \Big) \Delta(\mathbf{r}),$$
$$\hat{K}(\varepsilon_n, \sigma) = \mathcal{G}_{\varepsilon_n, \sigma}(\mathbf{p})\, \mathcal{G}_{-\varepsilon_n, -\sigma}(-\mathbf{p} + \mathbf{\Pi}), \quad (4)$$

where $\mathcal{G}_{\varepsilon_n, \sigma}(\mathbf{p}) = (i\varepsilon_n - \xi(\mathbf{p}) + \sigma h)^{-1}$ is the Fourier transform of $\mathcal{G}_{\varepsilon_n, \sigma}(\mathbf{r})$, ε_n is a fermionic Matsubara frequency, and $\mathbf{\Pi} = -i\nabla + 2|e|\mathbf{A}$. The full expression for the quartic term is given in the supplementary information [26].

The effects due to small ring size $R \sim \xi_0$ are contained in the discrete sum over integers m in $\sum_{\mathbf{p}}$. We use the Poisson summation formula [8], $\sum_{m \in Z} \delta(x - m) = \sum_{k \in Z} e^{i 2\pi k x}$ to elucidate these effects: $k = 0$ gives the continuum result for a 2D superconductor, and higher order terms, $k \geq 1$, account for the finite size corrections. After a straightforward calculation, we find

$$a^{(2)}(l, q_z, T, H) \simeq \frac{M}{2\pi} \Bigg[\ln\Big(\frac{T}{T_c}\Big) + \psi\Big(\frac{1}{2}\Big) - \frac{1}{4} \sum_{s_\varepsilon, \sigma = \pm 1} \int_0^{2\pi} \frac{d\varphi_p}{2\pi} \psi\Big(\frac{1}{2} - \frac{i s_\varepsilon}{4\pi T}\big[2\sigma h - \mathbf{v}_F \cdot \mathbf{Q}\big]\Big) \quad (5)$$
$$+ 2 \sum_{k>0} \int_0^{2\pi} \frac{d\varphi_p}{2\pi} \cos\Big(2\pi k\, R\, p_F \cos(\varphi_p)\Big) \sum_{n>0} \Big(\frac{e^{-\frac{R}{\xi_0}\pi(2n+1)k|\cos(\varphi_p)|}}{n + \frac{1}{2}} - \frac{1}{4} \sum_{s_\varepsilon, \sigma} \frac{e^{-\frac{R}{\xi_0}\frac{T}{T_c}\pi(2n+1)k|\cos(\varphi_p)|}}{n + \frac{1}{2} - \frac{i s_\varepsilon}{4\pi T}[2\sigma h - \mathbf{v}_F \cdot \mathbf{Q}]} \Big) \Bigg],$$

where we defined the product

$$\mathbf{v}_F \cdot \mathbf{Q} = 2\pi T_c \Big(\xi_0 q_z \sin(\varphi_p) + \Big[l - \frac{\Phi}{\Phi_0}\Big] \frac{\xi_0}{R} \cos(\varphi_p) \Big). \quad (6)$$

Here, $\psi(z)$ is the digamma function and the Fermi momentum is $p_F = \sqrt{2M\mu}$. In the second line of Eq. (5) we neglected terms of order T_c^2/μ^2. Because of the exponential decay of the terms with increasing $k > 0$ in the last term of Eq. (5), below we keep only the first finite size correction, $k = 1$. We checked that incorporating higher k does not qualitatively change our results.

Fig. 2 shows the upper critical field and the parameters l, q_z of the modulation of the superconducting order parameter at transition. Hereafter we consider $\xi_0 p_F = 100$, and $R \simeq 3\xi_0$. In the cylindrical geometry the inhomogeneous superconducting states emerge even for the materials that do not support FFLO modulation in the bulk: we present the results for the paramagnetic parameter $\alpha_M = g\mu_B \Phi_0/(\pi \xi_0^2 T_c) = 0.6$, which corresponds to the

Pauli limiting field $H_P \approx 4H_{c2}^{\text{orb}}$, so that the bulk material is a conventional orbital-limited type-II superconductor. The scalloped shape of the boundary of the superconducting region is the consequence of the LP effect, and the overall suppression of T_c with increased field is due to the paramagnetic pairbreaking. Below a characteristic temperature, which is non-universal and different from the $T^\star = 0.56T_{c0}$ for bulk Pauli limited superconductors, the inhomogeneous pairing along the cylinder axis ($q_z \neq 0$) becomes advantageous, and the FFLO state appears.

Fig. 2 shows that the modulation wave vector, q_z, along the transition line exhibits a "sawtooth" pattern, quite distinct from the uniform increase in q in the standard picture of Pauli-limited superconductors. This feature is due to the effective discretization of the modulation in Eq. (6). For a 2D sheet the role of the winding number l is taken by a continuous variable q_x, and it is the net $q = \sqrt{q_z^2 + q_x^2}$ that ensures matching of the energy of the

two electrons in a Cooper pair with the center of mass momentum q. In contrast, in the cylindrical geometry the choice of l is determined by the net flux, Φ, and therefore the momentum q_z adjusts to this selection, and exhibits discontinuities at the points where transitions between winding numbers l and $l+1$ occur. The detailed balance between q_z and l depends on the finite size quantum correction term, second line in Eq. (5). Note that the prefactor of the first non-vanishing k term, $\cos[2\pi R\,p_F\cos(\varphi_p)]$, has the same angle-dependence in the momentum space as the LP term, $|l - \Phi/\Phi_0|\cos(\varphi_p)/R$, and is out of phase with the FFLO modulation that enters with $\sin(\varphi_p)$ in Eq. (6). Consequently the details of the switching between values of l and q_z depend on the value of Rp_F (close to integer vs. half-integer), but the qualitative pic-
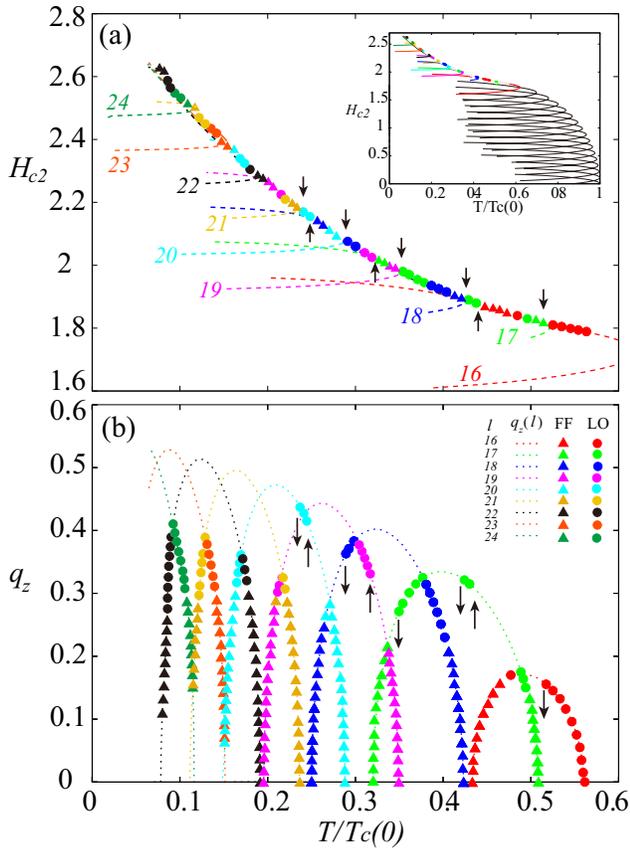

FIG. 3: (Color online) The specific heat jump at the onset of the modulated SC order in field, $\Delta C(T_c(H))/T_c(H)$. The notations are the same as in Fig.2. Inset: the same over the entire temperature range of the superconducting transition. The non-monotonous behavior appears *only* for the FFLO state, $q_z \neq 0$.

ture remains unchanged.

The discontinuous behavior of the modulation $q_z(T)$ is reflected in the experimental properties that allow unambiguous determination of the modulated state. Fig. 3 shows the specific heat jump at the superconducting transition for different fields. We verified that the quartic term, $a^{(4)}(l, q_z, T_c(H), H)$, remains positive along the entire transition line, and therefore the transition is always of second order. The favored state is determined by comparing the magnitude of the quartic term for the FF and the LO states: A smaller value corresponds to the greater condensation energy and a more stable phase. We find that in the vicinity of the discontinuous drop of the modulation q_z the FF state is favored, and is superseded by the LO state as q_z increases within the realm of each fixed winding number l. The specific heat jump at the transition is given by (we omit full labels for brevity) $\Delta C/T_c(H) = ([a^{(2)}]')^2/2a^{(4)}$ evaluated at $T_c(H)$, where $[a^{(2)}]' = (\partial a^{(2)}/\partial T)$. The heat capacity exhibits significant enhancement on transitions between different winding numbers. It is important to note that this non-monotonous behavior of the specific heat jump only appears when the transition is into FFLO state, at low temperatures and high fields. At higher T, when the transition is into the superconducting state with $q_z = 0$, the specific heat jump at the transition varies smoothly, see the inset of Fig. 3. The enhancement of the specific heat jump in the hollow cylinder geometry can be detected, for example, by the ac calorimetry technique, and therefore can serve as experimental proof of the existence of the FFLO-like modulations of the superconducting order in mesoscopic cylinders.

FIG. 2: (Color online) Structure of the modulated state for $R/\xi_0 = 3$ and $\alpha = 0.6$. (a) The upper critical fields H_{c2} normalized by $\Phi_0/\pi\xi_0^2$. Inset and dashed lines show $H_{c2}(T)$ for a given angular momentum l pairing state as indicated. Solid symbols denote the physical transition. Note the switching between the FF (triangles) and LO (circles) states along the transition line. (b) FFLO modulation wave vector q_z normalized by $1/\xi_0$ for each l (dotted lines), and at the physical transition as in panel (a). The circles (triangles) denote the stability regions of the LO (FF) state. Note the non-analytic behavior of q_z exhibiting kinks and discontinuous jumps at temperatures denoted by arrows.
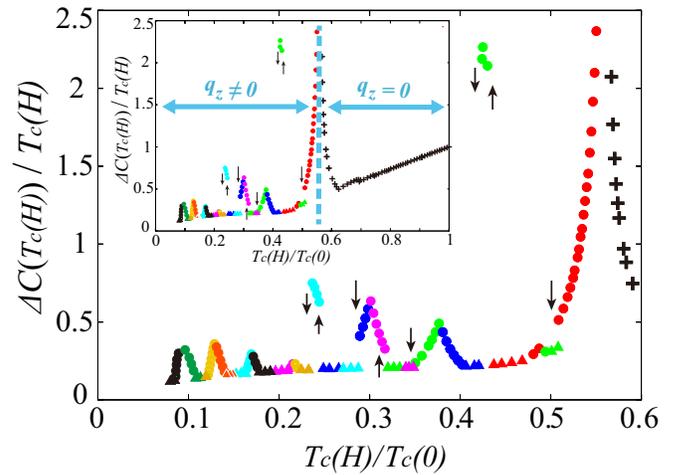
It is likely that in the experimental realization of the proposed geometry the superconductor will be disordered. We checked that the modulated states, and the non-monotonic behavior of $q_z(T)$ are robust against moderate impurity scattering [26] The former result is consistent with the conclusions of Refs. 29, 30. FFLO modulation disappears at strong disorder when transport becomes diffusive [28].

To conclude, we find novel spatially-inhomogeneous superconducting states, exhibiting both the Little-Parks and FFLO phenomenology, can emerge due to the vector potential and Zeeman coupling induced by a magnetic field threading a thin hollow cylinder. Our principal motivation was conventional superconductors, for which the coherence length can be well in excess of 1000Å. In this setting, the relevant sample sizes are experimentally accessible and we believe that the predicted variations in the specific heat jump can be found under realistic conditions, providing a possible "smoking-gun" experiment for detecting the FFLO state. In principle, cold atomic gases in a cylindrical geometry and coupled to a light-induced artificial magnetic field could realize a similar phase diagram and FFLO state [31]. However, given the difficulty of directly measuring the heat-capacity jump in a trapped cold atomic gas, it may currently be easier to detect the effects in small-size superconducting systems.

---

[1] R. E. Prange and S. M. Girvin, *The Quantum Hall Effect* (Springer, New York, 1987).

[2] S. M. Reimann and M. Manninen, Rev. Mod. Phys. **74**, 1283 (2002).

[3] M. Z. Hasan and C. L. Kane, Rev. Mod. Phys. **82**, 3045 (2010).

[4] K. T. Law, P. A. Lee, and T. K. Ng, Phys. Rev. Lett. **103**, 237001 (2009).

[5] W. A. Little and R. D. Parks, Phys. Rev. Lett. **9**, 9 (1962).

[6] Y. Liu, Yu. Zadorozhny, M. M. Rosario, B. Y. Rock, P. T. Carrigan, and H. Wang, Science **294**, 2332 (2001).

[7] E. N. Bogachek, G. A. Gogadze, and I. O. Kulik, Phys. Status Solidi B **67**, 287 (1975).

[8] T.-C. Wei and P. M. Goldbart, Phys. Rev. B **77**, 224512 (2008).

[9] P. Fulde and R. A. Ferrell, Phys. Rev. **135**, A550 (1964).

[10] A. I. Larkin and Yu. N. Ovchinnikov, Sov. Phys. JETP **20**, 762 (1965).

[11] A. Bianchi, R. Movshovich, C. Capan, P. G. Pagliuso, and J. L. Sarrao, Phys. Rev. Lett. **91**, 187004 (2003).

[12] T. Watanabe, Y. Kasahara, K. Izawa, T. Sakakibara, Y. Matsuda, C. J. van der Beek, T. Hanaguri, H. Shishido, R. Settai, and Y. Onuki, Phys. Rev. B **70**, 020506(R) (2004).

[13] K. Kumagai, M. Saitoh, T. Oyaizu, Y. Furukawa, S. Takashima, M. Nohara, H. Takagi, and Y. Matsuda, Phys. Rev. Lett. **97**, 227002 (2006); K. Kumagai, H. Shishido, T. Shibauchi, Y. Matsuda, Phys. Rev. Lett. **106**, 137004 (2011).

[14] J. Singleton, J. A. Symington, M.-S. Nam, A. Ardavan, M. Kurmoo, and P. Day, J. Phys. Condens. Matter **12**, L641 (2000).

[15] S. Uji, T. Terashima, M. Nishimura, Y. Takahide, T. Konoike, K. Enomoto, H. Cui, H. Kobayashi, A. Kobayashi, H. Tanaka, M. Tokumoto, E. S. Choi, T. Tokumoto, D. Graf, and J. S. Brooks, Phys. Rev. Lett. **97**, 157001 (2006).

[16] K. Cho, B. E. Smith, W. A. Coniglio, L. E. Winter, C. C. Agosta, and J. A. Schlueter, Phys. Rev. B **79**, 220507(R) (2009).

[17] S. Yonezawa, S. Kusaba, Y. Maeno, P. Auban-Senzier, C. Pasquier, K. Bechgaard, and D. Jerome, Phys. Rev. Lett. **100** 117002 (2008).

[18] Y. Matsuda and H. Shimahara, J. Phys. Soc. Jpn **76**, 051005 (2007).

[19] Under special assumptions about pairing interactions, multiple Fourier components of l may coexist at the transition, see, for example, F. Loder, A. P. Kampf, and T. Kopp, arXiv:1212.2429 (unpublished).

[20] H. Shimahara, J. Phys. Soc. Jpn. **67** 736 (1998).

[21] R. Combescot and C. Mora, Phys. Rev. B **71** 144517 (2005); 214504 (2005).

[22] M. Houzet and A. Buzdin, Phys. Rev. B **63**, 184521 (2001).

[23] H. Adachi and R. Ikeda, Phys. Rev. B **68**, 184510 (2003).

[24] N. Hiasa, T. Saiki, and R. Ikeda, Phys. Rev. B **80**, 014501 (2009).

[25] L. Radzihovsky, Phys. Rev. A **84**, 023611 (2011).

[26] K. Aoyama et al., supplementary information.

[27] A. A. Zyuzin and A. Yu. Zyuzin, Phys. Rev. B **79**, 174514 (2009).

[28] L. G. Aslamazov, Zh. Eksp. Teor. Fiz. **55**, 1477 (1968) [Sov. Phys. JETP **28**, 773 (1969)].

[29] D. F. Agterberg and K. Yang, J. Phys.: Condens. Matter **13**, 9259 (2001).

[30] A. B. Vorontsov, I. Vekhter, and M. J. Graf, Phys. Rev. B **78**, 180505(R) (2008).

[31] Y.-J. Lin, R.L. Compton, A.R. Perry, W.D. Phillips, J.V. Porto, and I.B. Spielman, Phys. Rev. Lett. **102**, 130401 (2009).

[32] L. Radzihovsky and D.E. Sheehy, Rep. Prog. Phys. **73**, 076501 (2010).